Walisongo Journal of Chemistry Vol. 8 Issue 1 (2025), 87-97
ISSN: 2621-5985 (online); 2549-385X (print)
DOI: https://doi.org/10.21580/wjc.v8i1.25826

MALACHITE GREEN TRANSPORT USING POLYMER INCLUSION MEMBRANE METHOD WITH co-EDVB AS CARRIER

Kharisma Citra Aprilia*[1], *Nurul Ulfa Safitri*[1], *Khusna Arif Rakhman*[2], *Agung Abadi Kiswandono*[1]

[1]Department of Chemistry, Faculty of Mathematics and Natural Sciences, Universitas Lampung, Lampung, Indonesia
[2]Department of Chemistry Education, Faculty of Teacher Training and Education, Universitas Khairun, Ternate, Indonesia

*Corresponding author: agung.abadi@fmipa.unila.ac.id

Abstract

Malachite green (MG) is a synthetic dye known for its toxic and carcinogenic properties, necessitating effective removal from aquatic environments. This study investigated the use of a polymer inclusion membrane (PIM) containing co-poly(eugenol-divinylbenzene) (co-EDVB) 2% as a carrier for the selective transport of MG. The membrane was prepared by dissolving co-EDVB, polyvinyl chloride, and dibenzyl ether in tetrahydrofuran (THF). Several parameters were evaluated, including the pH of the source phase, the concentration of nitric acid in the receiving phase, membrane thickness, carrier concentration, transport time, and competitive transport in synthetic wastewater. UV-Visible spectrophotometric analysis at a wavelength of 613 nm revealed that the transport efficiency reached 90.95% under optimal conditions: source phase pH 7, 0.50 M HNO_3 *in the receiving phase, membrane thickness* T_{54}*, and 18 hours of transport. In the presence of competing metal ions such as* Pb^{2+} *and* Cu^{2+}*, the efficiency decreased to 80.79%, confirming the important role of co-EDVB in enhancing transport selectivity and efficiency.*

Keywords: *Copoly Eugenol Divinyl Benzene, Malachite Green, Polymer Inclusion Membrane, Selective Transport, Wastewater.*

Introduction

The rapid growth of the industrial sector has led to environmental degradation and pollution, including hazardous industrial waste such as synthetic dyes (Khan et al., 2023; Uddin, 2021). These dyes, particularly those from the textile industry, are non-biodegradable and contain heavy metals like arsenic, lead, and mercury, posing toxic and carcinogenic risks (Soo et al., 2021).

Malachite green (MG) is a widely used synthetic dye due to its low cost and durability. However, it is classified as harmful by the US Food and Drug Administration (FDA) and by the Ministerial Decree of the Indonesian Ministry of Marine Affairs and Fisheries No. 52/KEPMEN-KP/2014. To mitigate its risks, the permissible concentration is limited to 0.01 ppm, necessitating effective wastewater treatment methods. Its discharge into water bodies reduces light penetration, threatens aquatic ecosystems, and has carcinogenic, mutagenic, and teratogenic effects (Sharma & Sharma, 2023).

Several treatment methods have been explored, including adsorption by microalgae biochar (Pathy et al., 2022), photocatalysis (Sarathi et al., 2023), and ionic flocculation (Teixeira et al., 2022). However, many of these methods merely transfer pollutants between phases without fully resolving environmental issues (He et al., 2023; Kiswandono et al., 2022). Liquid membrane technology is an effective method for removing hazardous pollutants through selective transport across a membrane interface, minimizing secondary pollution and offering a more sustainable alternative to conventional treatments (Kiswandono et al., 2024; Yusuf et al., 2020).

Among various liquid membrane systems, polymer inclusion membranes (PIM) have demonstrated significant advantages due to their high stability, reusability, and selectivity in the transport of contaminants such as MG (Kaczorowska et al., 2023; Kiswandono et al., 2024). Incorporating polyvinyl chloride (PVC) within the membrane matrix enhances stability by minimizing carrier loss and facilitating selective transport with low energy consumption (Khairati et al., 2025; Khalid et al., 2022). Previous studies have explored various carriers for MG transport using PIM. Kiswandono et al. (2024) investigated polyeugenol as a carrier, but its limited cross-linking capacity resulted in suboptimal long-term stability (Kiswandono et al., 2022; Saka et al., 2020). Similarly, Khairati et al. (2025) employed copoly(eugenol-diallyl phthalate) 2%, which exhibited moderate selectivity but did not achieve optimal transport efficiency for MG.

The present study explored the use of co-poly(eugenol-divinylbenzene) (co-EDVB) 2% as an alternative carrier for MG transport in PIM, building upon previous studies utilizing polymer-based carriers. Compared to other carriers such as polyeugenol or copoly(eugenol-diallyl phthalate), co-EDVB offers enhanced molecular stability and improved transport efficiency due to the presence of divinyl benzene (DVB), facilitating stronger cross-linking within the polymer matrix. Eugenol derived from clove leaf oil, undergoes polymerization to form polyeugenol, while divinyl benzene (DVB) enhances molecular integrity through cross-linking (Prasetya et al., 2020).

Co-EDVB serves as a pivotal carrier within the polymer inclusion membrane (PIM) system by forming a highly cross-linked polymeric network that substantially enhances the membrane's structural integrity, chemical resilience, and functional selectivity. The copolymerization of eugenol, which is rich in phenolic hydroxyl and allyl functional groups, with divinylbenzene (DVB) yields a robust three-dimensional matrix (Kiswandono et al., 2022). This matrix exhibits superior mechanical strength and chemical stability, particularly under acidic conditions commonly employed in the receiving phase. The phenolic moieties of eugenol engage in π–π stacking and hydrogen bonding interactions with the aromatic ring system of MG, thereby facilitating selective molecular recognition and transport. Concurrently, DVB acts as an effective cross-linker that mitigates carrier leaching and degradation, prolonging membrane lifespan and operational efficiency. The synergistic effect of these components results in a PIM with enhanced transport performance, even in complex matrices containing competing metal ions, thus positioning co-EDVB as a multifunctional carrier with selective and stabilizing properties (Kiswandono et al., 2023).

This structural modification results in improved chemical resistance, mechanical strength, and enhanced MG transport efficiency. Compared to previously studied carriers, co-EDVB 2% exhibits superior durability, reduced degradation, and higher selectivity in MG transport.

Methodology

Tools and materials

The instruments used in this study included a UV-Vis spectrophotometer (Shimadzu 1800), operated at a wavelength of 613 nm, to determine the concentration of malachite green (MG) in the source and receiving phases. Fourier Transform

Infrared Spectroscopy (FT-IR, Cary 630) was employed to identify functional groups in the membrane, with a scanning range of 4000–650 cm^{-1} and a resolution of 4 cm^{-1}. Scanning Electron Microscopy-Energy Dispersive X-ray (SEM-EDX, ZEISS EVO MA 10) was operated at an accelerating voltage of 20 kV under high vacuum mode to observe the membrane's surface morphology and elemental composition. A pH meter (Hanna Instruments HI 83141) was calibrated using standard buffer solutions at pH 4.01 and 7.00 prior to measurement. Other supporting equipment included an analytical digital balance (Mettler Toledo AB54-S) with ±0.1 mg readability, a magnetic stirrer and bar for homogeneous mixing, and a thickness gauge (Ghatin) for measuring membrane thickness. Additional glassware and accessories included a membrane mold (5 cm), separatory funnel, stand and clamp, round-bottom flask, volumetric flask, measuring cylinder, beaker, dropper pipette, mortar and pestle, spatula, stirring rod, aluminum foil, and tissue.

The materials used in this study included MG ($C_{52}H_{54}N_4O_{12}$, molar mass 927.00 g/mol, purity ≥ 90%, Sigma-Aldrich, CAS No. 2437-29-8), Eugenol ($C_{10}H_{12}O_2$, molar mass 164.20 g/mol, purity ≥ 99%, Sigma-Aldrich, CAS No. 97-53-0), and Polyvinyl Chloride (PVC) with a density of 1.1–1.35 g/cm^3 (analytical grade, Sigma-Aldrich, CAS No. 9002-86-2). Additional materials included Dibenzyl Ether (DBE) ($C_{14}H_{14}O$, molar mass 198.28 g/mol, purity ≥ 98%, Sigma-Aldrich, CAS No. 103-50-4), Tetrahydrofuran (THF) (C_4H_8O, molar mass 72.11 g/mol, purity ≥ 99.9%, Merck, CAS No. 109-99-9), and Nitric Acid (HNO_3) (molar mass 63.01 g/mol, 65% w/w, Merck, CAS No. 7697-37-2). Other reagents included Lead(II) Carbonate ($PbCO_3$) (molar mass 267.21 g/mol, analytical grade, Sigma-Aldrich, CAS No. 598-63-0), Copper(II) Nitrate Trihydrate ($Cu(NO_3)_2 \cdot 3H_2O$) (molar mass 241.60 g/mol, purity ≥ 98%, Merck, CAS No. 10031-43-3), and Divinylbenzene (DVB) ($C_{10}H_{10}$, molar mass 130.19 g/mol, purity ≥ 98%, Sigma-Aldrich, CAS No. 132174-0). Distilled water and aquadest were used throughout all solution preparations.

Determination of Maximum Wavelength of Malachite Green (MG)

Before measuring MG concentration, the maximum absorbance wavelength of 25 ppm MG was determined using a UV-Vis spectrophotometer within the wavelength range of 400–800 nm (Kiswandono et al., 2024).

Variation of Malachite Green (MG) pH in the Source Phase

The PIM containing the carrier compound was placed in a transport tube. Then, 50 cm^3 of 1 M HNO_3 (receiving phase) and 50 cm^3 of 25 ppm MG at pH values of 5, 6, 7, 8, and 9 (source phase) were added. The tube was sealed and stirred for 12 hours. Subsequently, 5 cm^3 samples from both phases were collected, and MG concentrations were measured using a UV-Vis spectrophotometer (Kiswandono et al., 2024).

Variation of HNO_3 Concentration in the Receiving Phase

Different concentrations of HNO_3 (0.50, 0.75, 1.00, 1.25, and 1.50 M) were prepared by diluting 13 M HNO_3. Specific volumes of 9.6 cm^3, 14.4 cm^3, 19.2 cm^3, 24 cm^3, and 28.8 cm^3 were pipetted into 250 cm^3 volumetric flasks and diluted to the mark with distilled water. The PIM with the carrier compound was placed in the transport tube, followed by the addition of 50 cm^3 of the respective HNO_3 solution (receiving phase) and 50 cm^3 of 25 ppm MG at the optimal pH (source phase). The tube was sealed and stirred for 12 hours. Afterward, 5 cm^3 samples from both phases were collected, and MG concentrations were measured using a UV-Vis spectrophotometer (Kiswandono et al., 2024).

Variation of Membrane Thickness

PIM membranes with varying thicknesses (T_{27}, T_{54}, and T_{108}), each containing the carrier compound, were placed in the transport tube. Subsequently, 50 cm^3 of HNO_3 (at its optimum concentration) and 50 cm^3 of 25 ppm MG solution (at its optimum pH) were added as the receiving and source phases, respectively. The tube was sealed and stirred for 12 hours. After stirring, 5 cm^3 fractions were separately collected from the source and receiving phases to analyze the MG concentration. Measurements were performed using a UV-Vis spectrophotometer (Kiswandono et al., 2024). The composition of membrane-forming components used to produce the different membrane thicknesses is presented in Table 1.

Table 1. Composition of co-poly(eugenol-divinylbenzene) (co-EDVB)-based membrane-forming components (Kiswandono et al., 2022)

Type	co-EDVB (g)	Polyvinyl Chloride (g)	Dibenzyl Ether (g)	Total Weight (g)
T_{27}	0.027	0.087	0.156	0.27
T_{54}	0.054	0.173	0.313	0.54
T_{108}	0.108	0.346	0.626	1.08

Variation of Carrier Compound Concentration

A PIM membrane of standard thickness (T_{54}) with varying concentrations of the carrier compound (Table 1) was placed in the transport tube. Then, 50 cm^3 of HNO_3 (at the optimum concentration) was added as the receiving phase, and 50 cm^3 of 25 ppm MG (at the optimum pH) as the source phase. The tube was sealed and stirred for 12 hours. Afterward, 5 cm^3 samples were collected from both phases, and the concentrations of MG were measured using a UV-Vis spectrophotometer (Kiswandono et al., 2024).

Variation of Transport Time

A PIM membrane with standard thickness was positioned at the center of the transport tube. A 50 cm^3 solution of HNO_3 (at its optimum concentration) was used as the receiving phase, while a 50 cm^3 solution of 25 ppm MG (at its optimum pH) served as the source phase. The tube was sealed and stirred using a magnetic stirrer for different durations: 6, 12, 18, 24, and 30 hours. At the end of each time interval, 5 cm^3 samples were taken from both the source and receiving phases. The concentration of MG in each phase was then analyzed using a UV-Vis spectrophotometer at the maximum absorption wavelength.

Results and Discussion

PIM Membrane Preparation

The PIM membrane was prepared using a specialized mold equipped with a magnetic stirrer. The membrane composition included co-EDVB (carrier), PVC (base polymer), and DBE (plasticizer). The resulting membrane is shown in Figure 1.

Figure 1. PIM membrane containing co-EDVB

The membrane exhibited a yellowish color, was elastic in nature, and had a diameter of approximately 3 cm. These physical characteristics suggest successful membrane formation and good homogeneity. The carrier facilitated transport, the polymer provided mechanical support, and the plasticizer enhanced flexibility and overall stability.

Transport of Malachite Green (MG) at Varying pH in the Source Phase

The transport efficiency of MG was evaluated at source phase pH values of 5, 6, 7, 8, and 9. At lower pH values (5 and 6), transport efficiency was relatively low, likely due to a reduced chemical potential gradient and the competitive presence of H^+ ions, inhibiting the interaction between MG and the membrane phase. The effect of source phase pH variation is illustrated in Figure 2.

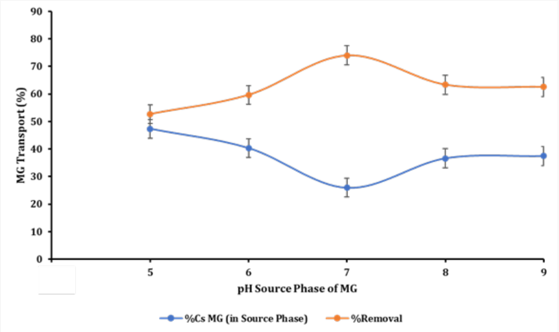

Figure 2. Effect of source phase pH on the concentration of Malachite Green transported

At pH 7, transport efficiency increased significantly, reaching 74.28%. This enhancement was attributed to MG predominantly existing in its molecular form at this pH, allowing for stronger π–π interactions and hydrogen bonding within the membrane phase, thereby facilitating transport (Zhao & Zhu, 2020).

However, as the pH increased to 8 and 9, a gradual decrease in transport efficiency was observed. This decline might be due to MG deprotonation or partial degradation under alkaline conditions, which weakened π–π interactions and reduced adsorption efficiency (Xu et al., 2024). Among the tested values, pH 7 emerged as the most favorable for MG transport. This finding aligns with prior studies supporting near-neutral pH as optimal for the source phase (Kiswandono et al., 2024). The effective pH range for MG transport has generally been reported between 2 and 10 (Jalilvand et al., 2020).

Transport of Malachite Green (MG) at Varying HNO_3 Concentrations in the Receiving Phase

Optimal MG transport was observed at a receiving phase HNO_3 concentration of 0.50 M, achieving a removal efficiency of 81.49%, as shown in Figure 3. This suggests that a moderate acid concentration promoted efficient MG extraction by enhancing electrostatic and hydrophilic interactions without introducing excessive ion competition or saturation.

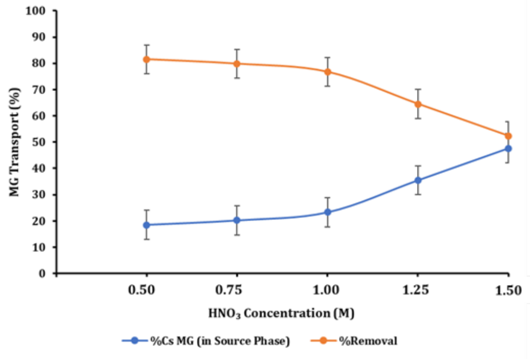

Figure 3. Effect of HNO_3 concentration in the receiving phase on the concentration of Malachite Green transported

MG transport was affected by the concentration of HNO_3, which dissociated into NO_3^- and H_3O^+ ions. As a cationic dye, MG interacted favorably with the hydrophilic environment of the receiving phase, especially in the presence of H_3O^+, enhancing its mobility and facilitating membrane transport. At higher HNO_3 concentrations, however, transport efficiency declined, likely due to an imbalance between the acid concentration and the amount of MG released (Kiswandono et al., 2024).

Kiswandono et al. (2024) reported optimal conditions using PIM with polyeugenol as the carrier at 0.75 M HNO_3, while Khairati et al. (2025) found a similar optimum at 0.75 M HNO_3 using copoly-eugenol-diallyl-phthalate as the carrier.

Variation of Membrane Thickness

PIM membranes of varying thicknesses (T_{27}, T_{54}, and T_{108}) were evaluated for MG transport using 0.50 M HNO_3 as the receiving phase and 25 ppm MG at pH 7 as the source phase. After 12 hours of transport, it was evident that membrane thickness significantly affected removal efficiency: T_{27} achieved 71.44%, T_{54} reached 82.11%, and T_{108} yielded 61.12%.

Among these, the T_{54} membrane demonstrated optimal performance by balancing molecular interactions and carrier distribution. The improved transport efficiency at this thickness could be attributed to the effective interaction between MG molecules and the carrier compound, resulting in a membrane that was neither too dense nor too porous (Kiswandono et al., 2024). These findings are summarized in Table 4 and visually represented in Figure 4.

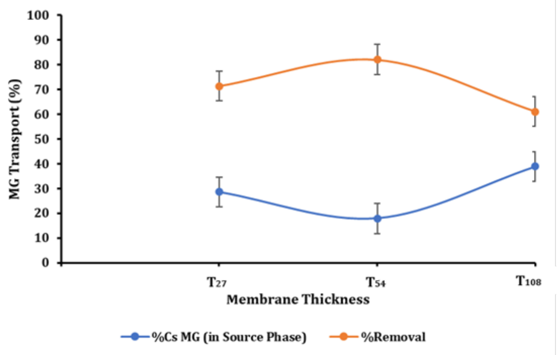

Figure 4. Effect of PIM membrane thickness on the transported concentration of Malachite Green

The data indicate that PIM membrane thickness played a critical role in MG transport efficiency. Thickness, measured in millimeters using a gauge, affected the amount of carrier and the membrane's mechanical properties. The thinnest membrane (T_{27}) might have limited carrier content, resulting in competition among MG molecules for interaction sites. On the other hand, the thickest membrane (T_{108}) might restrict diffusion due to increased rigidity and a higher concentration of components, which could inhibit molecular mobility and decrease transport performance (Khairati et al., 2025).

Variation in Carrier Compound Concentration

The effect of varying co-EDVB concentrations on MG transport was studied under optimized conditions. The removal efficiencies observed were 79.34% (0.01 M), 86.59% (0.02 M), 64.68% (0.03 M), 58.26% (0.04 M), and 55.17% (0.05 M). The correlation between carrier concentration and MG transport efficiency is illustrated in Figure 5.

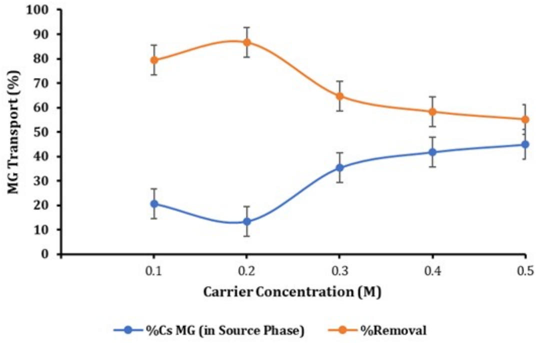

Figure 5. Effect of carrier compound concentration on the transported concentration of Malachite Green

The highest removal efficiency (86.59%) was achieved at a co-EDVB concentration of 0.02 M. At this level, the increased availability of –OH active sites enhanced π-π interactions between MG and DVB, facilitating effective transport. However, at concentrations ≥ 0.03 M, the %removal declined. This drop could be attributed to the excessive presence of active sites, leading to molecular competition and overlapping interaction zones within the membrane. Such site saturation reduced the efficiency of MG uptake and hindered its transport across the membrane (Kiswandono et al., 2024; Saka et al., 2020).

Variation in Transport Time

Transport time is a key factor affecting MG interaction with the carrier compound, primarily through hydrogen bonding and π–π interactions. Prolonged contact time strengthens these interactions, thus enhancing the transfer of MG to the receiving phase (Khairati et al., 2025). The impact of varying transport durations is shown in Figure 6.

The optimal transport duration was found to be 18 hours, achieving a peak removal efficiency of 90.95%. The %removal values at different time intervals were as follows: 56.10% (6 hours), 71.44% (9 hours), 88.40% (12 hours), and 60.75% (24 hours). Although prolonged transport time can enhance membrane–solute interactions, an excessive duration (e.g., 24 hours) may lead to a decline in performance. This drop is likely due to the degradation of the liquid membrane (LM), resulting in the leaching of membrane components and a consequent reduction in active sites (Khairati et al., 2025; Kiswandono et al., 2024). Furthermore, saturation of HNO_3 in the receiving phase might limit further uptake of MG, thereby diminishing overall transport efficiency.

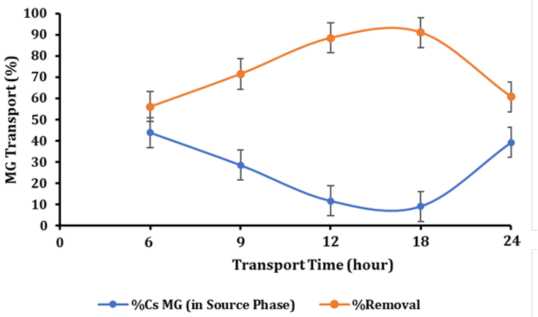

Figure 6. Effect of time variation on the concentration of transported Malachite Green

Membrane Characterization

Membrane characterization was done using FT-IR and SEM-EDX. FT-IR analysis was used to identify the functional groups involved in the transport process, while SEM-EDX provided insight into the surface morphology and elemental composition of the membrane post-transport (Figure 7).

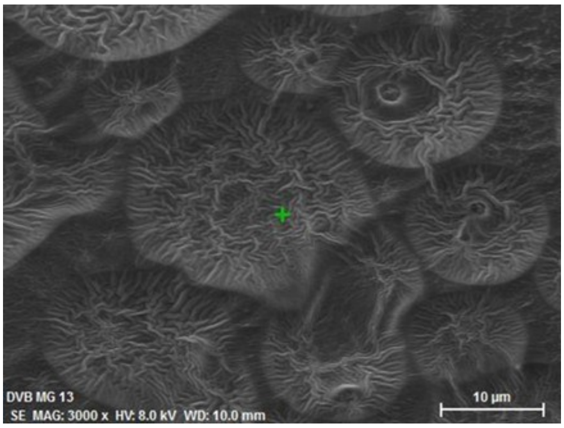

Figure 7. Surface morphology of the membrane after Malachite Green transport in synthetic waste

SEM-EDX analysis confirmed the presence of heavy metals, specifically Cu(II) and Pb(II), on the membrane surface after the transport process. The detection of these metals in the receiving phase indicates their partial uptake or interaction during the MG transport cycle. The respective concentrations of these heavy metals, identified through EDS analysis, are shown in Figure 8.

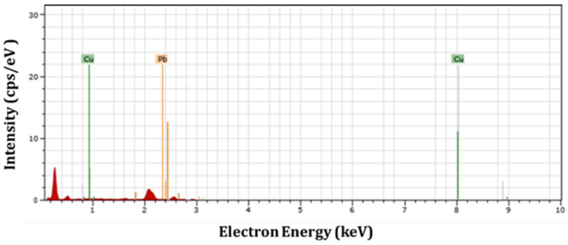

Figure 8. EDS spectrum of the membrane after Malachite Green transport in synthetic waste

According to Figure 8, the EDS spectrum analysis results show that the percentage of Cu(II) metal was 2.80% and the percentage of Pb(II) metal was 14.34%, both obtained from the membrane after the transport of MG in synthetic waste. The presence of these metals affected the transport of MG. In addition to the SEM-EDX characterization after transport, FT-IR characterization was also performed on the metal variations. The FT-IR characterization in this study aimed to identify the functional groups present in the PIM membrane after the transport of MG in synthetic waste. The presence of Pb(II) and MG+Cu(II) + Pb(II) can be observed in the infrared spectra shown in Figure 9.

The interaction between the PIM membrane and metals occurred when metals adhered to the membrane during the MG transport process, which could be observed from the results of the infrared spectra. This interaction led to changes in wave numbers and intensities on the membrane, indicating that Cu(II) and Pb(II) metals had interacted with the membrane, although the interaction was weak (Mancilla-Rico & Rodríguez, 2022). The infrared absorption spectra of the membrane after MG transport and the membrane after synthetic wastewater transport can be seen in Table 2. Table 2 shows that the FT-IR analysis results of the membrane after MG transport (MG control) and the membrane after transport with synthetic wastewater did not show significant differences in wave numbers. This was due to the interaction of Cu(II) and Pb(II) metal ions with the carrier compounds on the membrane, forming complex compounds that obstructed the interaction between active groups, such as the -OH group of the carrier compounds on the membrane (Macías & Rodríguez, 2023). Each metal interacting with the membrane imparts its own characteristics when interacting with the carrier compounds.

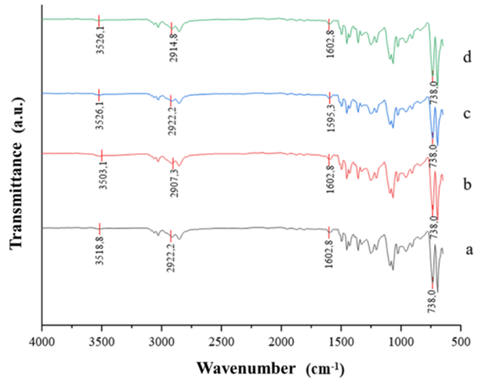

Figure 9. Comparison of FT-IR spectra of the membrane after transport: (a) Control MG, (b) MG and Cu(II) metal, (c) MG and Pb(II) metal, and (d) MG, Cu(II) metal, and Pb(II) metal.

Table 2. Comparison of wave numbers of the membrane after Malachite Green transport

Functional Groups	**Wavenumber (cm^{-1}) Membrane after transport**			
	Malachite Green	**Malachite Green+Pb**	**Malachite Green+Cu**	**Malachite Green+Pb+Cu**
Hydrogen-bonded alcohol (–OH)	3518.8	3503.1	3526.1	3526.1
Csp^3–H Stretching (–CH3)	2922.2	2907.3	2922.2	2914.8
Aromatic (C=C)	1602.8	1602.8	1595.3	1602.8
Aromatic (C–H)	738.0	738.0	738.0	738.0

Conclusion

Based on the results obtained, it can be concluded that the transport of malachite green (MG) reached its optimum conditions at a source phase pH of 7, a receiving phase concentration of 0.50 M, and a membrane thickness of T_{54} over an 18-hour transport period. This resulted in a 90.95% removal of MG to the receiving phase. The presence of Cu(II) and Pb(II) metals in synthetic wastewater was found to disrupt the transport of MG, reducing the removal efficiency to 87.93%. When these metals acted as competitors, the MG transport efficiency further decreased to 80.79%, with Cu(II) and Pb(II) concentrations reaching 2.80% and 14.24%, respectively in the receiving phase. Characterization of the PIM membrane using SEM after transport showed surface irregularities and pore formation, likely due to the partial loss of membrane components (leaching). Additionally, FT-IR analysis revealed minor shifts and slight decreases in absorption band intensities, which might indicate molecular interactions or structural changes within the membrane during the transport process, although these differences were not significantly pronounced.

Acknowledgments

The authors would like to express gratitude to the Ministry of Education, Culture, Research, and Technology for the financial support provided through the 2024 Master's Thesis Research grant (Master's contract number

057/E5/PG.02.00.PL/2024, dated June 11, 2024), and the Derivative contract number 574/UN26.21/PN/2024, dated June 19, 2024

References

Abhijeet Pathy, Nageshwari Krishnamoorthy, Scott X. Chang, B.P. (2022) 'Malachite green removal using algal biochar and its composites with kombucha SCOBY: An integrated biosorption and phycoremediation approach', *Surfaces and Interfaces*, 30, p. 101880. Available at: https://doi.org/https://doi.org/10.1016/j.surfin.2022.101880.

Candra Saka, Agung Abadi Kiswandono, S.H. (2020) 'Synthesis Of Polymer Inclusion Membranes Based On Pvc Containing Copoly-Edvb 4% As A Carrier For Removal Of Phenol Solutions', *Pollution Research Journal*, 39(4), pp. 1009–1016. Available at: https://www.envirobiotechjournals.com/PR/v39i420/Poll Res-25.pdf.

Faheem Uddin (2021) 'Environmental hazard in textile dyeing wastewater from local textile industry', *Cellulose*, 28, pp. 10715–10739. Available at: https://doi.org/https://doi.org/10.1007/s10570-021-04228-4.

Guoke Zhao, H.Z. (2020) 'Cation–π Interactions in Graphene-Containing Systems for Water Treatment and Beyond', *Advanced materials*, 33(2), p. 1905756. Available at: https://doi.org/https://doi.org/10.1002/adma.201905756.

He, J., Mo, P., Luo, Y. S., & Yang, P. H. (2023). Strategies for solving the issue of malachite green residues in aquatic products: A review. *Aquaculture Research*, 2023(1), 8578570. https://doi.org/10.1155/2023/8578570

Jalilvand, P., Rahbar-Kelishami, A., Mohammadi, T., & Shayesteh, H. (2020). Optimizing of malachite green extraction from aqueous solutions using hydrophilic and hydrophobic nanoparticles. *Journal of Molecular Liquids*, 308, 113014. https://doi.org/10.1016/j.molliq.2020.113014

Kaczorowska, M. A., Bożejewicz, D., & Witt, K. (2023). The application of polymer inclusion membranes for the removal of emerging contaminants and synthetic dyes from aqueous solutions—A mini review. *Membranes*, 13(2), 132. https://doi.org/10.3390/membranes13020132

Khairati, R. M., Kiswandono, A. A., Rinawati, R., & Ma'ruf, D. I. (2025). Application of polymer inclusion membrane in the transport of malachite green dye using copolymer (eugenol-diallyl phthalate) 2% as a carrier. *Jurnal Kimia Sains dan Aplikasi*, 28(1), 8–15. https://doi.org/10.14710/jksa.28.1.8-15

Khalid, N., Shoparwe, N., Yusoff, A., Sulaiman, A., Ahmad, A., & Azmi, N. (2022). Fabrication and characterisation of MWCNT/polyvinyl (PVC) polymer inclusion membrane for zinc (II) ion removal from aqueous solution. *Membranes*, 12(10). https://doi.org/10.3390/membranes12101020

Khan, W. U., Ahmed, S., Dhoble, Y., & Madhav, S. (2023). A critical review of hazardous waste generation from textile industries and associated ecological impacts. *Journal of the Indian Chemical Society*, 100(1), 100829. https://doi.org/10.1016/j.jics.2022.100829

Kiswandono, A. A., Antika, W., Rahmawati, A., & Rinawati, R. (2023). Investigating phenol transport using copoly (eugenol-DVB) 8% as a carrier with the supported liquid membrane method. *Jurnal Kimia Sains dan Aplikasi*, 26(10), 372–380. https://doi.org/10.14710/jksa.26.10.372-380

Kiswandono, A. A., Sindiani, A. V., Khotimah, R. K., Rabbani, M. B., Kurniawan, B., Rinawati, R., & Putra, H. E. (2024). Transport of malachite green using the polyeugenol-based polymer inclusion membrane (PIM) method. *Journal of Membrane Science and Research*, 10(1), 1–5. https://doi.org/10.22079/JMSR.2023.2013382.1635

Kiswandono, A. A., Widiarto, S., Sari, D. T. E. N., Supriyanto, R., Qudus, H. I., Rinawati, R., ... & Devariani, W. (2022). Kompetisi fenol pada limbah buatan menggunakan kopoli-eugenol divinil benzena 10% sebagai senyawa pembawa. *ALCHEMY Jurnal Penelitian Kimia*, 18(1), 1–9. https://doi.org/10.20961/alchemy.18.1.45356.1-9

Kiswandono, A., Aprilia, K., Rahmawati, A., Widiarto, S., & Rinawati, R. (2024). Evaluation of polymer inclusion membrane containing copoly eugenol divinyl benzene 10% as a carrier for phenol transport. *Journal of Advanced Research in Fluid Mechanics and Thermal Sciences*, 122(2), 38–51. https://doi.org/10.37934/arfmts.122.2.3851

Kiswandono, A., Nusantari, C., Rinawati, R., & Hadi, S. (2022). Optimization and evaluation of polymer inclusion membranes based on PVC containing copoly-EDVB 4% as a carrier for the removal of phenol solutions. *Membranes*, 12, 1–13. https://doi.org/10.3390/membranes12030295

Macías, M., & Rodríguez de San Miguel, E. (2023). On the use of polymer inclusion membranes for the selective separation of Pb(II), Cd(II), and Zn(II) from seawater. *Membranes*, 13(5), 512. https://doi.org/10.3390/membranes13050512

Mancilla-Rico, A. J., & Rodríguez de San Miguel, E. (2022). Simultaneous determination of Cu(II), Zn(II), and Pb(II) from aqueous solutions using a polymer inclusion membrane (PIM) based-sensor with 1-(2-pyridylazo)-2-naphthol (PAN) as chromophore and chemometric methods. *Frontiers in Analytical Science*, 2, 971352. https://doi.org/10.3389/frans.2022.971352

Pathy, A., Krishnamoorthy, N., Chang, S. X., & Paramasivan, B. (2022). Malachite green removal using algal biochar and its composites with kombucha SCOBY: An integrated biosorption and phycoremediation approach. *Surfaces and Interfaces*, 30, 101880. https://doi.org/10.1016/j.surfin.2022.101880

Prasetya, N. B. A., Ngadiwiyana, N., Ismiyarto, I., & Sarjono, P. R. (2020). Effects of percent weight of divinylbenzene as crosslinking agent on the properties of eugenol–divinylbenzene copolymers. *Journal of Physics: Conference Series*, 1524(1), 012089. https://doi.org/10.1088/1742-6596/1524/1/012089

Sarathi, R., Devi, L. R., Sheeba, N. L., Esakki, E. S., & Sundar, S. M. (2023). Photocatalytic degradation of malachite green dye by metal oxide nanoparticles—mini review. *Journal of Chemical Reviews*, 5(1), 15–30. https://doi.org/10.22034/JCR.2023.359935.1187

Sharma, J., Sharma, S., & Soni, V. (2023). Toxicity of malachite green on plants and its phytoremediation: A review. *Regional Studies in Marine Science*, 62, 102911. https://doi.org/10.1016/j.rsma.2023.102911

Soo, J. A. L., Makhtar, M. M. Z., Shoparwe, N. F., Otitoju, T. A., Mohamad, M., Tan, L. S., & Li, S. (2021). Characterization and kinetic studies of poly(vinylidene fluoride-co-hexafluoropropylene) polymer inclusion membrane for the malachite green extraction. *Membranes*, 11(9), 676. https://doi.org/10.3390/membranes11090676

Teixeira, Y. N., Melo, R. P. F., Fernandes, M. R., Carmo, S. K. S., & Neto, E. B. (2022).

Malachite green removal using ionic flocculation. *Water Practice and Technology*, 17(5), 1113–1128. https://doi.org/10.2166/wpt.2022.054

Uddin, F. (2021). Environmental hazard in textile dyeing wastewater from local textile industry. *Cellulose*, 28(17), 10715–10739. https://doi.org/10.1007/s10570-021-04228-4Zhao, G., & Zhu, H. (2020). Cation–π interactions in graphene-containing systems for water treatment and beyond. *Advanced Materials*, 32(22), 1905756. https://doi.org/10.1002/adma.201905756

Xu, Y., Zhang, J., Jia, G., Ji, D., Ding, Y., & Zhao, P. (2024). Evaluating malachite green removal from aqueous solution by hydroxyl enhanced hydrochar and biomass. *Biomass Conversion and Biorefinery*, 14(13), 14391–14404. https://doi.org/10.1007/s13399-022-03647-y

Yusuf, A., Sodiq, A., Giwa, A., Eke, J., Pikuda, O., De Luca, G., ... & Chakraborty, S. (2020). A review of emerging trends in membrane science and technology for sustainable water treatment. *Journal of Cleaner Production*, 266, 121867. https://doi.org/10.1016/j.jclepro.2020.121867